5382 *Inorg. Chem.* **2009**, *48*, 5382–5391
DOI: 10.1021/ic900454g

Inorganic Chemistry
Article

Volatility and High Thermal Stability in Tantalum Complexes Containing Imido, Amidinate, and Halide or Dialkylamide Ligands

Monika K. Wiedmann, Mary Jane Heeg, and Charles H. Winter*

Department of Chemistry, Wayne State University, Detroit, Michigan 48202

Received March 7, 2009

Treatment of Ta(NtBu)Cl$_3$(py)$_2$ with 2 equiv of Li(iPrNCMeNiPr) or Li(tBuNCMeNtBu) afforded Ta(NtBu)(iPrNCMeNiPr)$_2$Cl and Ta(NtBu)(tBuNCMeNtBu)$_2$Cl in 63% and 61% yields, respectively. Treatment of Ta(NtBu)(iPrNCMeNiPr)$_2$Cl or Ta(NtBu)(tBuNCMeNtBu)$_2$Cl with LiNRR′ afforded Ta(NtBu)(iPrNCMeNiPr)$_2$(NRR′) and Ta(NtBu)(tBuNCMeNtBu)$_2$(NRR′) in 79−92% yields (R, R′ = Me, Et). Treatment of Ta(NtBu)(tBuNCMeNtBu)$_2$Cl with AgBF$_4$ afforded Ta(NtBu)(tBuNCMeNtBu)$_2$F in 54% yield, while treatment of Ta(NtBu)(tBuNCMeNtBu)$_2$Cl with BBr$_3$ afforded Ta(NtBu)(tBuNCMe-NtBu)$_2$Br in 68% yield. X-ray crystal structures of Ta(NtBu)(tBuNCMeNtBu)$_2$F and Ta(NtBu)(tBuNCMeNtBu)$_2$Br revealed that the amidinate ligands exhibit η^2-coordination, and that the imido and halide ligands are *cis* to each other within the distorted octahedral structures. NMR studies indicated that the other complexes have analogous structures. Additionally, variable temperature NMR studies revealed that some of the complexes undergo amidinate rearrangement. The enthalpies, entropies, and free energies of activation for these rearrangements were calculated for Ta(NtBu)(tBuNCMeNtBu)$_2$X (X = F, Cl, Br). When X = F, $\Delta H^{\ddagger} = 9.1 \pm 0.4$ kcal/mol, $\Delta S^{\ddagger} = -20.5 \pm 1.6$ cal/mol·K, and $\Delta G^{\ddagger}$(298 K) = 15.3 ± 0.7 kcal/mol. For X = Cl, $\Delta H^{\ddagger} = 12.4 \pm 0.3$ kcal/mol, $\Delta S^{\ddagger} = -20.2 \pm 0.8$ cal/mol·K, and $\Delta G^{\ddagger}$(298 K) = 18.4 ± 0.3 kcal/mol. When X = Br, $\Delta H^{\ddagger} = 12.5 \pm 0.5$ kcal/mol, $\Delta S^{\ddagger} = -21.7 \pm 1.5$ cal/mol·K, and $\Delta G^{\ddagger}$(298 K) = 19.0 ± 0.7 kcal/mol. All of the complexes are volatile, and they sublime between 120 and 203 °C. In addition, Ta(NtBu)(iPrNCMeNiPr)$_2$NMe$_2$ has a decomposition point that is 65−160 °C higher than widely used film growth precursors and is therefore a promising candidate for use in chemical vapor deposition and atomic layer deposition film growth techniques.

Introduction

Thin films of tantalum-based materials have a variety of applications. Ta$_2$O$_5$ has a high dielectric constant and has been explored for application in microelectronics devices as the gate dielectric in metal-oxide-semiconductor field effect transistors and as the capacitor dielectric in dynamic random access memories.[1,2] Ta$_2$O$_5$ has also been used in antireflective coatings,[3] waveguides for light,[4] electrochromic devices,[5] ion-sensitive field effect transistors,[6] humidity sensors,[7] and as a barrier material in magnetic tunnel junctions.[8] TaN is one of the best diffusion barrier materials between silicon and copper.[9−11] SrBi$_2$Ta$_2$O$_9$ is a ferroelectric material that has been extensively investigated for nonvolatile ferroelectric memory applications.[12] Pb(Sc$_{0.5}$Ta$_{0.5}$)O$_3$ exhibits pyroelectric and ferroelectric properties.[13] The ongoing miniaturization of features in microelectronics devices requires the growth of these materials as thin, conformal films. Two methods for depositing thin films are chemical vapor deposition[14] (CVD)

---

*To whom correspondence should be addressed. E-mail: chw@chem.wayne.edu.

(1) Chaneliere, C.; Autran, J. L.; Devine, R. A. B.; Balland, B. *Mater. Sci. Eng. R* **1998**, *22*, 269–322.

(2) Yoon, D.-S.; Roh, J. S.; Baik, H. K.; Lee, S.-M. *Crit. Rev. Solid State Mater. Sci.* **2002**, *27*, 143–226.

(3) (a) Janicki, V.; Sancho-Parramon, J.; Stenzel, O.; Lappschies, M.; Görtz, B.; Rickers, C.; Polenzky, C.; Richter, U. *Appl. Opt.* **2007**, *46*, 6084–6091. (b) Janicki, V.; Gäbler, D.; Wilbrandt, S.; Leitel, R.; Stenzel, O.; Kaiser, N.; Lappschies, M.; Görtz, B.; Ristau, D.; Rickers, C.; Vergöhl, M. *Appl. Opt.* **2006**, *45*, 7851–7857. (c) Koc, K.; Tepehan, F. Z.; Tepehan, G. G. *J. Mater. Sci.* **2005**, *40*, 1363–1366.

(4) (a) Lahoz, F.; Shepherd, D. P.; Wilkinson, J. S.; Hassan, M. A. *Opt. Commun.* **2008**, *281*, 3691–3694. (b) Schmitt, K.; Schirmer, B.; Hoffmann, C.; Brandenburg, A.; Meyrueis, P. *Biosens. Bioelectron.* **2007**, *22*, 2591–2597.

(5) (a) Tai, C.-Y.; Wu, J.-Y. *J. Phys. D: Appl. Phys.* **2008**, *41*, 065303. (b) Ozer, N.; Lampert, C. M. *J. Sol-Gel Sci. Technol.* **1997**, *8*, 703–709.

(6) Kwon, D.-H.; Cho, B.-W.; Kim, C.-S.; Sohn, B.-K. *Sens. Actuators B* **1996**, *34*, 441–445.

(7) (a) Kimura, M. *Sens. Actuators A* **1996**, *55*, 7–11. (b) Eranna, G.; Joshi, B. C.; Runthala, D. P.; Gupta, R. P. *Crit. Rev. Solid State Mater. Sci.* **2004**, *29*, 111–188.

(8) Gillies, M. F.; Kuiper, A. E. T.; van Zon, J. B. A.; Sturm, J. M. *Appl. Phys. Lett.* **2001**, *78*, 3496–3498.

(9) Winter, C. H. *Aldrichim. Acta* **2000**, *33*, 3–12.

(10) Singer, P. *Semicond. Int.* **2002**, *25*(5), 46–53.

(11) Peters, L. *Semicond. Int.* **2003**, *26*(3), 50–54.

(12) (a) Whittle, K. R.; Hyatt, N. C.; Reaney, I. M. *Chem. Mater.* **2008**, *20*, 6427–6433. (b) Condorelli, G. G.; Favazza, M.; Bedoya, C.; Baeri, A.; Anastasi, G.; Lo Nigro, R.; Menou, N.; Muller, C.; Lisoni, J. G.; Wouters, D.; Fragalà, I. L. *Chem. Mater.* **2006**, *18*, 1016–1022. (c) Schumacher, M.; Lindner, J.; Baumann, P. K.; Schienle, F.; Solayappan, N.; Joshi, V.; Araujo, C. A.; McMillan, L. D. *Mater. Sci. Semicond. Proc.* **2003**, *5*, 85–91. (d) Ramesh, R.; Aggarwal, S.; Auciello, O. *Mater. Sci. Eng. R* **2001**, *32*, 191–236. (e) Paz, C. A.; Cuchiaro, J. D.; McMillan, L. D.; Scott, M. C.; Scott, J. F. *Nature* **1995**, *374*, 627–629.

(13) (a) Lan, D.; Xiao, D.; Xu, Z.; Chen, Y.; Chen, Q.; Yue, X.; Zhu, J. *J. Electroceram.* **2008**, *21*, 621–624. (b) Huang, Z.; Donohue, P. P.; Zhang, Q.; Williams, D.; Anthony, C. J.; Todd, M. A.; Whatmore, R. W. *Integr. Ferroelectr.* **2002**, *45*, 79–87.

(14) (a) Pierson, H. O. *Handbook of Chemical Vapor Deposition (CVD)*; Noyes Publications/William Andrew Publishing: Norwich, NY, 1999. (b) Hitchman, M. L.; Jenson, K. F. Chemical Vapor Deposition: Principles and Applications; Academic Press: London, 1993.

and atomic layer deposition[15] (ALD). In CVD, one or more gaseous precursors is introduced into the deposition chamber. If a single source is used, the film is grown by thermal decomposition of the precursor on the substrate; if two or more precursors are employed, reactions between them can occur both in the gas phase and on the substrate surface, resulting in a film. ALD differs from CVD in that the precursors are introduced into the reaction chamber in alternate pulses, with an inert gas purge between each pulse to clear the reaction chamber of excess precursor as well as reaction byproducts. Thereby, gas phase reactions are eliminated, and the self-limited process forms conformal films whose thickness can be accurately controlled by the number of deposition cycles. Requirements for ALD precursors are different than those of CVD precursors.[15] ALD precursors must be sufficiently volatile, thermally stable at the deposition temperature, and must react with a second precursor to form the desired thin film.[15] Metal halides have been frequently employed as ALD precursors, since they generally possess volatility and high thermal stability. However, they release corrosive hydrogen halides upon treatment with water or ammonia and can cause halogen contamination of the growing film. To eliminate these problems, recent research has been directed toward the development of halogen-free metalorganic ALD precursors. $Ta(OEt)_5$,[16] $Ta(NMe_2)_5$,[17] $Ta(NEt)(NEt_2)_3$,[17a] $Ta(NtBu)(NEt_2)_3$,[18] and $Ta(NtBu)(tBu_2pz)_3$[19] have been used for the growth of Ta_2O_5, TaN, or Ta_3N_5 films by ALD. However, most of these precursors have limited thermal stability, which restricts self-limited ALD growth to moderate temperatures. For example, $Ta(OEt)_5$ undergoes thermal decomposition at 275 °C,[16b] and self-limited growth with $Ta(NMe_2)_5$[17] and $Ta(NtBu)(NEt_2)_3$[18b,18c] is lost above 250 °C because of precursor thermal decomposition. $Ta(NtBu)(tBu_2pz)_3$ has extraordinary thermal stability and exhibits self-limited ALD growth between 300 and 450 °C.[19] However, its low reactivity requires ozone as the oxygen source to form Ta_2O_5. The deposition of tantalum nitride presents an additional challenge, since most often the insulating Ta_3N_5 phase is formed, rather than the desired conducting TaN phase, unless an additional reducing agent is used in conjunction with ammonia.[20,21]

Amidinate ligands have been coordinated to metals across the periodic table.[22,23] Amidinate ligands usually exhibit the η^2-coordination mode to a single metal center, and their steric and electronic properties can be adjusted by varying the substituents on the core nitrogen and carbon atoms. Recently, d-block and lanthanide complexes containing amidinate ligands have been used as precursors in ALD.[24] Also, tantalum complexes containing the related guanidinate ligands have been explored as potential precursors in the CVD growth of tantalum nitride.[25,26] Many tantalum complexes containing amidinate ligands have been reported,[27] but none has been used as a precursor in ALD or CVD depositions.

Tantalum complexes containing imido ligands are plentiful.[28] Imido ligands have been incorporated into many

---

(15) (a) Ritala, M.; Leskelä, M. In *Handbook of Thin Film Materials*; Nalwa, H. S., Ed.; Academic Press: San Diego, CA, 2002; Vol. 1, pp 103−159. (b) Leskelä, M.; Ritala, M. Angew. Chem., Int. Ed. 2003, 42, 5548–5554. (c) Niinist, L.; Päiväsaari, J.; Niinist, J.; Putkonen, M.; Nieminen, M. Phys. Status Solidi A 2004, 201, 1443–1452. (d) Putkonen, M.; Niinist, L. Top. Organomet. Chem. 2005, 9, 125–145.

(16) (a) Kukli, K.; Ritala, M.; Leskelä, M. *J. Electrochem. Soc.* **1995**, *142*, 1670–1675. (b) Kukli, K.; Aarik, J.; Aidla, A.; Siimon, H.; Ritala, M.; Leskelä, M. *Appl. Surf. Sci.* **1997**, *112*, 236–242. (c) Rahtu, A.; Kukli, K.; Ritala, M. *Chem. Mater.* **2001**, *13*, 817–823. (d) Alén, P.; Vehkamäki, M.; Ritala, M.; Leskelä, M. *J. Electrochem. Soc.* **2006**, *153*, G304–G308.

(17) (a) Hausmann, D. M.; de Rouffignac, P.; Smith, A.; Gordon, R.; Monsma, D. *Thin Solid Films* **2003**, *443*, 1–4. (b) Maeng, W. J.; Kim, H. *Electrochem. Solid-State Lett.* **2006**, *9*, G191–G194. (c) Maeng, W. J.; Park, S.-J.; Kim, H. *J. Vac. Sci. Technol. B* **2006**, *24*, 2276–2281.

(18) (a) van der Straten, O.; Zhu, Y.; Dunn, K.; Eisenbraun, E. T.; Kaloyeros, A. E. *J. Mater. Res.* **2004**, *19*, 447–453. (b) Burton, B. B.; Lavoie, A. R.; George, S. M. *J. Electrochem. Soc.* **2008**, *155*, D508–D516. (c) Song, M.-K.; Rhee, S.-W. *J. Electrochem. Soc.* **2008**, *155*, H823–H828.

(19) Dezelah, C. L.IV; Wiedmann, M. K.; Mizohata, K.; Baird, R. J.; Niinistö, L.; Winter, C. H. *J. Am. Chem. Soc.* **2007**, *129*, 12370–12371.

(20) (a) Hiltunen, L.; Leskelä, M.; Makelä, M.; Niinistö, L.; Nykänen, E.; Soinen, P. *Thin Solid Films* **1988**, *166*, 149–154. (b) Fix, R.; Gordon, R. G.; Hoffman, D. M. *Chem. Mater.* **1993**, *5*, 614–619. (c) Winter, C. H.; Jayaratne, K. C.; Proscia, J. W. *Mater. Res. Soc. Syp. Proc.* **1994**, *327*, 103–108. (d) Han, C.-H.; Cho, K.-N.; Oh, J.-E.; Paek, S.-H.; Park, C.-S.; Lee, S.-I.; Lee, M. Y.; Lee, J. G. *Jpn. J. Appl. Phys.* **1998**, *37*, 2646–2651. (e) Cho, K.-N.; Han, C.-H.; Noh, K.-B.; Oh, J.-E.; Paek, S.-H.; Park, C.-S.; Lee, S.-I.; Lee, M. Y.; Lee, J. G. *Jpn. J. Appl. Phys.* **1998**, *37*, 6502–6505. (f) Jun, G.-C.; Cho, S.-L.; Kim, K.-B.; Shin, H.-K.; Kim, D.-H. *Jpn. J. Appl. Phys.* **1998**, *37*, L30–L32. (g) Ritala, M.; Kalsi, P.; Riihelä, D.; Kukli, K.; Leskelä, M.; Jokinen, J. *Chem. Mater.* **1999**, *11*, 1712–1718. (h) Kim, H.; Lavoie, C.; Copel, M.; Narayanan, V.; Park, D.-G.; Rossnagel, S. M. *J. Appl. Phys.* **2004**, *95*, 5848–5855. (i) Wu, Y. Y.; Kohn, A.; Eizenberg, M. *J. Appl. Phys.* **2004**, *95*, 6167–6174. (j) Lehn, J.-S. M.; van der Heide, P.; Wang, Y.; Suh, S.; Hoffman, D. M. *J. Mater. Chem.* **2004**, *14*, 3239–3245. (k) Kim, D.-K.; Kim, B.-H.; Woo, H.-G.; Kim, D.-H.; Shin, H. K. *J. Nanosci. Nanotechnol.* **2006**, *6*, 3392–3395. (l) Chung, H.-S.; Kwon, J.-D.; Kang, S.-W. *J. Electrochem. Soc.* **2006**, *153*, C751–C754.

(21) For a review of TaN_x by ALD, see: Kim, H. *J. Vac. Sci. Technol. B* **2003**, *21*, 2231−2261, and references therein.

(22) For a review, see: Barker, J.; Kilner, M. *Coord. Chem. Rev.* **1994**, *133*, 219–300.

(23) For recent selected examples, see: (a) Schmidt, J. A. R.; Arnold, J. *Chem. Commun.* **1999**, 2149–2150. (b) Foley, S. R.; Yap, G. P. A.; Richeson, D. S. *Organometallics* **1999**, *18*, 4700–4705. (c) Foley, S. R.; Zhou, Y.; Yap, G. P. A.; Richeson, D. S. *Inorg. Chem.* **2000**, *39*, 924–929. (d) Blais, P.; Chivers, T.; Downard, A.; Parvez, M. *Can. J. Chem.* **2000**, *78*, 10–15. (e) Dagorne, S.; Guzei, I. A.; Coles, M. P.; Jordan, R. F. *J. Am. Chem. Soc.* **2000**, *122*, 274–289. (f) Lim, B. S.; Rahtu, A.; Park, J.-S.; Gordon, R. G. *Inorg. Chem.* **2003**, *42*, 7951–7958. (g) Sadique, A. R.; Heeg, M. J.; Winter, C. H. *J. Am. Chem. Soc.* **2003**, *125*, 7774–7775.

(24) (a) Lim, B. S.; Rahtu, A.; Gordon, R. G. *Nat. Mater.* **2003**, *2*, 749–754. (b) Päiväsaari, J.; Dezelah, C. L.IV; Back, D.; El-Kaderi, H. M.; Heeg, M. J.; Putkonen, M.; Niinistö, L.; Winter, C. H. *J. Mater. Chem.* **2005**, *15*, 4224–4233. (c) de Rouffignac, P.; Park, J.-S.; Gordon, R. G. *Chem. Mater.* **2005**, *17*, 4808–4818. (d) Li, Z.; Rahtu, A.; Gordon, R. G. *J. Electrochem. Soc.* **2006**, *153*, C787–C794. (e) de Rouffignac, P.; Yousef, A. P.; Kim, K. H.; Gordon, R. G. *Electrochem. Solid State Lett.* **2006**, *9*, F45–F48.

(25) Baunemann, A.; Rische, D.; Milanov, A.; Kim, Y.; Winter, M.; Gemel, C.; Fischer, R. A. *Dalton Trans.* **2005**, 3051–3055.

(26) Baunemann, A.; Winter, M.; Csapek, K.; Gemel, C.; Fischer, R. A. *Eur. J. Inorg. Chem.* **2006**, 4665–4672.

(27) (a) Drew, M. G. B.; Wilkins, J. D. *J. Chem. Soc., Dalton Trans.* **1974**, 1579–1582. (b) Drew, M. G. B.; Wilkins, J. D. *J. Chem. Soc., Dalton Trans.* **1974**, 1973–1977. (c) Wilkins, J. D. *J. Organomet. Chem.* **1974**, *80*, 349–355. (d) Drew, M. G. B.; Wilkins, J. D. *J. Chem. Soc., Dalton Trans.* **1975**, 2611–2617. (e) Drew, M. G. B.; Wilkins, J. D. *Acta Crystallogr.* **1975**, *B31*, 177–182. (f) Drew, M. G. B.; Wilkins, J. D. *Acta Crystallogr.* **1975**, *B31*, 2642–2648. (g) Leboeuf, J. F.; Leblanc, J. C.; Moise, C. *J. Organomet. Chem.* **1987**, *335*, 331–337. (h) Cotton, F. A.; Matonic, J. H.; Murillo, C. A.; Wang, X. *Bull. Soc. Chim. Fr.* **1996**, *133*, 711–720. (i) Cotton, F. A.; Daniels, L. M.; Murillo, C. A.; Wang, X. *J. Am. Chem. Soc.* **1996**, *118*, 4830–4833. (j) Cotton, F. A.; Daniels, L. M.; Murillo, C. A.; Wang, X. *Inorg. Chem.* **1997**, *36*, 896–901. (k) Cotton, F. A.; Daniels, L. M.; Matonic, J. H.; Wang, X.; Murillo, C. A. *Polyhedron* **1997**, *16*, 1177–1191. (l) Dawson, D. Y.; Arnold, J. *Organometallics* **1997**, *16*, 1111–1113. (m) Decker, J. M.; Geib, S. J.; Meyer, T. Y. *Organometallics* **1999**, *18*, 4417–4420. (n) Chen, C.-T.; Doerrer, L. H.; Williams, V. C.; Green, M. L. H. *Dalton Trans.* **2000**, 967–974. (o) Chen, C.-T.; Rees, L. H.; Cowley, A. R.; Green, M. L. H. *Dalton Trans.* **2001**, 1761–1767. (p) Anderson, L. L.; Schmidt, J. A. R.; Arnold, J.; Bergman, R. G. *Organometallics* **2006**, *25*, 3394–3406. (q) Epshteyn, A.; Zavalij, P. Y.; Sita, L. R. *J. Am. Chem. Soc.* **2006**, *128*, 16052–16053.

(28) (a) Wigley, D. E. *Prog. Inorg. Chem.* **1994**, *42*, 239−482. (b) Bates, P. A.; Nielson, A. J.; Water, J. M. *Polyhedron* **1985**, *4*, 1391–1401.

CVD precursors to metal nitride films, since the strong metal–nitrogen bonds should remain intact during precursor decomposition, thereby assisting in the growth of metal nitride films.[29] ALD growth does not proceed by thermal decomposition,[15] so the presence of a strong tantalum–nitrogen triple bond in a precursor may not offer the same advantages as in CVD growth. However, we have demonstrated that Ta(NtBu)(tBu_2pz)$_3$ exhibits exceptional thermal stability,[19] and thus the presence of an alkyl imido ligand in an ALD precursor should help to confer thermal stability.

Herein we describe the synthesis, structure, and properties of a series of tantalum complexes of the formula Ta(NtBu)(RNCMeNR)$_2$X, where R is iPr or tBu and X is either halide or dialkylamide. These complexes undergo dynamic ligand exchange processes in solution, and the kinetics of these processes was studied using variable temperature NMR. The goal of this study was to prepare tantalum complexes that incorporate volatility and the highest possible thermal stability, and which possess high reactivity toward water to allow ALD growth with this oxygen source. The complexes reported herein are volatile, and sublime well at moderate temperatures with low residues. Thus, all of these complexes are potential CVD precursors. One of these complexes undergoes solid state decomposition at about 340 °C, which is much higher than existing metalorganic tantalum film growth precursors. This new complex thus may be a useful precursor for the ALD growth of tantalum-containing thin films.

Results

Synthetic Aspects. Treatment of Ta(NtBu)Cl$_3$(py)$_2$ with 2 equiv of Li(iPrNCMeNiPr) or Li(tBuNCMeNtBu) in toluene at ambient temperature afforded complexes **1** and **2** after workup, as described in the Experimental Section (eq 1). Both **1** and **2** are very soluble in hexane, but could be crystallized at −25 °C from concentrated solutions in 61–63% yields. The structural assignments were based upon spectral and analytical data. The ^{1}H NMR spectrum of **1** at 23 °C contains partially coalesced peaks because of rearrangement of the amidinate ligands on the NMR time scale. However, ^{1}H NMR spectra recorded at or below −10 °C showed sharp resonances, indicating that the ligand rearrangement is slow. The methyl protons of the four isopropyl groups appear as eight doublets, indicating that each methyl group is in a different chemical environment. Similarly, the methine protons of the isopropyl groups result in four septets, and the two methyl groups on the amidinate backbones each give rise to a singlet, while the *tert*-butyl group produces a singlet. These resonances imply that the chloride ion is *cis* to the *tert*-butylimido ligand, since this configuration contains four unique isopropyl groups. If the chloride ion were *trans* to the *tert*-butylimido ligand, all four isopropyl groups would be equivalent. Similarly, the ^{1}H NMR spectrum of **2** at 23 °C consists of five singlets for the five *tert*-butyl groups and two singlets for the two methyl groups, again indicating that the chloride ion and *tert*-butylimido ligand are *cis* to each other.

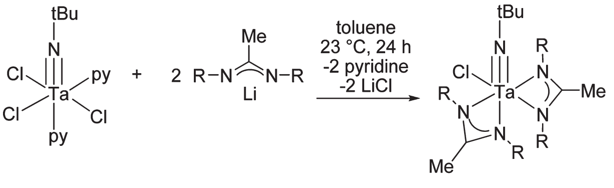

(1)

1, R = iPr, 63%
2, R = tBu, 61%

Treatment of **1** or **2** with lithium dimethylamide, lithium diethylamide, or lithium ethyl methylamide in tetrahydrofuran at ambient temperature afforded complexes **3**–**8** after workup, as outlined in eq 2. The structural assignments were based on spectral and analytical data. Complexes **4**, **6**, and **8** could be crystallized from hexane. All six complexes sublime readily, and this method of purification gave purer products in higher yields than crystallization from hexane. Like **1** and **2**, the ^{1}H NMR spectra of **3**–**8** contained unique resonances for each isopropyl and *tert*-butyl group, indicating that the dialkylamide and *tert*-butylimido ligands are *cis*. Additionally, the ^{1}H NMR spectra of **3** and **4** contained two singlets arising from the two chemically inequivalent methyl groups of the dimethylamide ligands. The ethyl groups in **5** and **6** afforded two triplets because of the methyl protons and four doublets of quartets arising from the diastereotopic methylene protons. In **7** and **8**, the ethyl methylamide ligand can adopt two different orientations, and thus each complex has two conformational isomers with different NMR resonances. Each isomer exhibits a singlet arising from the methyl group, as well as a triplet and two doublets of quartets because of the ethyl group. In benzene-d_6 solution at 23 °C, **7** consists of two isomers in a ratio of approximately 3:1, whereas **8** consists of two isomers in a ratio of approximately 2.3:1.

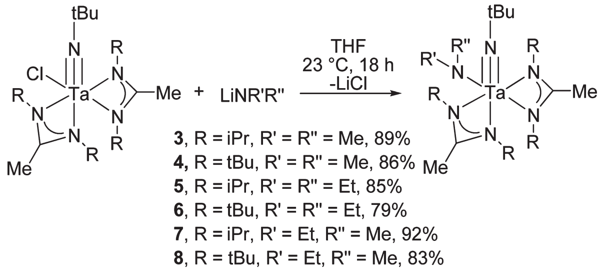

(2)

3, R = iPr, R' = R" = Me, 89%
4, R = tBu, R' = R" = Me, 86%
5, R = iPr, R' = R" = Et, 85%
6, R = tBu, R' = R" = Et, 79%
7, R = iPr, R' = Et, R" = Me, 92%
8, R = tBu, R' = Et, R" = Me, 83%

Treatment of **2** with $AgBF_4$ in dichloromethane at ambient temperature afforded **9** in 54% yield (eq 3), whereas treatment of **2** with BBr_3 in dichloromethane at ambient temperature afforded **10** in 68% yield (eq 4). The structural assignments were based on spectral and analytical data, as well as X-ray structure determinations. The ^{1}H NMR spectrum of **9** at 23 °C consisted of a sharp singlet due to the *tert*-butylimido group, two broad singlets arising from the four *tert*-butyl groups on the amidinate ligands, and two broad, partially coalesced singlets from the two methyl groups. As with **1**, the amidinate ligands in **9** undergo exchange on the NMR time scale, resulting in broad peaks. Below −20 °C, all of the *tert*-butyl and methyl groups appeared as sharp singlets. The ^{1}H NMR spectrum of **10** at 23 °C is analogous to that of **2**, and consists of seven sharp singlets – one for each methyl and *tert*-butyl group. Again,

---

(29) McElwee-White, L. *Dalton Trans.* **2006**, 5327–5333.

Table 1. Activation Parameters for **2**, **9**, and **10**

compound	$\Delta H^{\ddagger}$ (kcal/mol)	$\Delta S^{\ddagger}$ (cal/mol·K)	$\Delta G^{\ddagger}$(298 K) (kcal/mol)
Ta(NtBu)(tBuNCMeNtBu)$_2$F (**9**)	9.1 ± 0.4	−20.5 ± 1.6	15.3 ± 0.7
Ta(NtBu)(tBuNCMeNtBu)$_2$Cl (**2**)	12.4 ± 0.3	−20.2 ± 0.8	18.4 ± 0.3
Ta(NtBu)(tBuNCMeNtBu)$_2$Br (**10**)	12.5 ± 0.5	−21.7 ± 1.5	19.0 ± 0.7

this indicates that the halide ions and *tert*-butylimido ligands in **9** and **10** are *cis*, as was confirmed by their crystal structures.

(3)

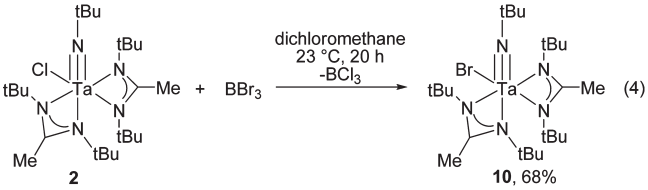

(4)

Kinetics Study. Since the ^{1}H NMR spectra of **1** and **9** at 23 °C showed broad resonances, indicating ligand exchange or rearrangement, several complexes were studied using variable temperature NMR to determine the exchange rates. The rates of ligand rearrangement were determined by line shape analysis, as described in the Experimental Section. Eyring plots gave the enthalpies and entropies of activation, and from these the free energies of activation were calculated (see Supporting Information). The results are summarized in Table 1.

Qualitatively, the ^{1}H NMR spectrum of **1** at ≤ -10 °C contained sharp resonances corresponding to the slow exchange limit. The methyl protons of the four isopropyl groups led to eight doublets, the methine protons of the isopropyl groups produced four septets, and the methyl groups on the amidinate backbones resulted in two singlets. Increasing the temperature resulted in broadened, partially coalesced peaks because of rearrangement of the diisopropylacetamidinate ligands on the NMR time scale. Upon reaching 78 °C, the ^{1}H NMR spectrum revealed one doublet corresponding to the methyl protons of the isopropyl groups, one septet due to the methine protons of the isopropyl groups, and one singlet from the methyl groups on the amidinate backbones. At all temperatures, the *tert*-butylimido resonance appeared as a sharp singlet. However, it was not possible to calculate the exchange rates because of the complex, overlapping resonances. For the same reason, the ligand exchange kinetics of other complexes containing diisopropylacetamidinate ligands was not studied.

The complexes containing di-*tert*-butylacetamidinate ligands were more amenable to kinetics analyses. Because of the greater steric bulk of the *tert*-butyl groups compared to the isopropyl groups, **2** did not show significant ligand rearrangement at 25 °C, but at higher temperatures, the peaks broaden and then coalesce, as depicted in Figure 1. Complex **10** shows behavior similar to that of **2**, except that the peaks broaden at slightly higher temperatures. Complex **9** exhibits broadened resonances at 23 °C. Complexes **4** and **6**, which contain dialkylamide ligands, do not show any significant line broadening even at 90 °C. Eyring analysis for **9** afforded $\Delta H^{\ddagger} = 9.1 \pm 0.4$ kcal/mol, $\Delta S^{\ddagger} = -20.5 \pm 1.6$ cal/mol·K, and $\Delta G^{\ddagger}$ (298 K) = 15.3 ± 0.7 kcal/mol. Related analysis for **2** gave $\Delta H^{\ddagger} = 12.4 \pm 0.3$ kcal/mol, $\Delta S^{\ddagger} = -20.2 \pm 0.8$ cal/mol·K, and $\Delta G^{\ddagger}$(298 K) = 18.4 ± 0.3 kcal/mol, while **10** showed $\Delta H^{\ddagger} = 12.5 \pm 0.5$ kcal/mol, $\Delta S^{\ddagger} = -21.7 \pm 1.5$ cal/mol·K, and $\Delta G^{\ddagger}$(298 K) = 19.0 ± 0.7 kcal/mol.

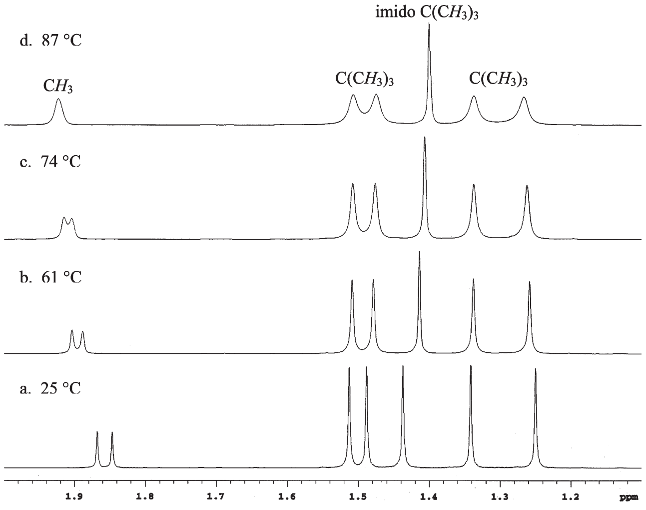

Figure 1. ^{1}H NMR spectra of Ta(NtBu)(tBuNCMeNtBu)$_2$Cl (**2**) at (a) 25 °C, (b) 61 °C, (c) 74 °C, and (d) 87 °C.

Volatility and Thermal Stability. The volatilities of **1**−**10** were evaluated by sublimation experiments. The crude solids were loaded into a horizontal sublimation apparatus and were sublimed in the range of 120 to 203 °C at a pressure of 0.05 Torr. All 10 complexes sublimed, with 64 to 94% recoveries starting from the crude reaction products. The ^{1}H NMR spectra of the sublimed compounds were identical to those of the materials prior to the sublimations. Additionally, preparative-scale sublimations (~0.7 g) were carried out on previously sublimed samples of **3** and **4**. These complexes sublimed at 154 and 169 °C with 88% and 96% recovery, respectively. There was < 1% nonvolatile residue left after each sublimation.

Complexes **1**−**10** were evaluated for thermal stability by heating a few milligrams of each sample in a sealed melting point capillary tube. Table 2 summarizes the decomposition temperatures. With the exception of **1** and **9**, all decompose without melting. Complex **1** melts with decomposition below 200 °C and is the least thermally stable of the series. Complex **9** melts without decomposition at 257−259 °C and undergoes thermal decomposition from 282 to 296 °C. The other halogen-containing complexes, **2** and **10**, decompose in the ranges of 260−270 °C and 213−228 °C, respectively. By

Table 2. Solid State Decomposition Temperatures of **1-10**

compound	decomposition range (°C)
1	161−206
2	260−270
3	324−340
4	298−309
5	244−259
6	298−301
7	300−322
8	297−306
9	282−296
10	213−228

Table 3. Crystal Data and Data Collection Parameters for **9** and **10**

	9	**10**
formula	$C_{24}H_{51}FN_5Ta$	$C_{24}H_{51}BrN_5Ta$
FW	609.65	670.56
space group	$P2_1/c$	$P2_1/n$
a (Å)	17.4098(5)	11.8983(4)
b (Å)	10.1352(3)	16.3458(6)
c (Å)	16.2928(5)	15.0157(5)
β (deg)	94.2780(10)	94.221(2)
V (Å^3)	2866.88(15)	2912.44(17)
Z	4	4
T (K)	100(2)	100(2)
λ (Å)	0.71073	0.71073
ρ_{calcd} (g, cm^{-3})	1.412	1.529
μ (mm^{-1})	3.859	5.165
R(F)^a	0.0237	0.0289
Rw(F)^b	0.0540	0.0716

[a] $R(F) = \sum||F_o| - |F_c||/\sum|F_o|$. [b] $Rw(F) = [\sum w(F_o^2 - F_c^2)^2/\sum w(F_o^2)^2]^{1/2}$, for $I > 2\sigma(I)$.

Table 4. Selected Bond Lengths (Å) and Angles (deg) for **9**

Ta−F	1.9434(16)	F−Ta−N(1)	101.27(9)
Ta−N(1)	1.797(2)	F−Ta−N(2)	146.04(8)
Ta−N(2)	2.1731(19)	F−Ta−N(3)	88.96(8)
Ta−N(3)	2.230(2)	F−Ta−N(4)	95.17(9)
Ta−N(4)	2.100(3)	F−Ta−N(5)	84.15(9)
Ta−N(5)	2.362(3)	N(1)−Ta−N(2)	98.44(9)
N(1)−C(1)	1.450(3)	N(1)−Ta−N(3)	102.59(9)
N(2)−C(5)	1.331(3)	N(1)−Ta−N(4)	103.08(11)
N(3)−C(5)	1.336(3)	N(1)−Ta−N(5)	162.94(11)
N(4)−C(15)	1.375(4)	N(2)−Ta−N(3)	59.74(8)
N(5)−C(15)	1.345(4)	N(2)−Ta−N(4)	106.96(9)
		N(2)−Ta−N(5)	85.02(8)
		N(3)−Ta−N(4)	152.63(11)
		N(3)−Ta−N(5)	93.61(9)
		N(4)−Ta−N(5)	60.09(10)
		Ta−N(1)−C(1)	170.1(2)
		N(2)−C(5)−N(3)	110.6(2)
		N(4)−C(15)−N(5)	111.2(2)

contrast, the dialkylamide-containing complexes **3**−**8** generally possess greater thermal stability. With the exception of **5**, which decomposes in the range of 244−259 °C, **3**, **4**, **6**, **7**, and **8** begin decomposing at or above 300 °C.

Structural Aspects. The X-ray crystal structures of **9** and **10** were determined to establish their solid-state structures. Experimental crystallographic data are summarized in Table 3, selected bond lengths and angles are given in Tables 4 and 5, and perspective views are presented in Figures 2 and 3.

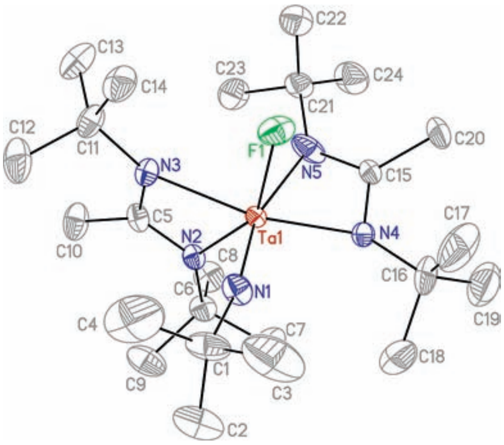

Figure 2. Perspective view of **9** showing only the major disorder component with thermal ellipsoids at the 50% probability level.

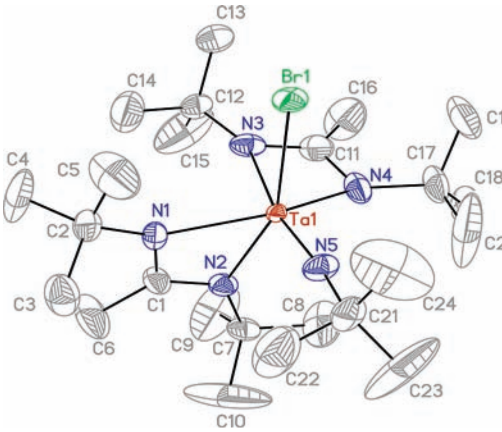

Figure 3. Perspective view of **10** showing only the major disorder component with thermal ellipsoids at the 50% probability level.

Table 5. Selected Bond Lengths (Å) and Angles (deg) for **10**

Ta−Br	2.565(2)	Br−Ta−N(1)	100.56(9)
Ta−N(1)	2.223(3)	Br−Ta−N(2)	156.85(11)
Ta−N(2)	2.171(3)	Br−Ta−N(3)	83.46(9)
Ta−N(3)	2.370(3)	Br−Ta−N(4)	92.51(10)
Ta−N(4)	2.074(3)	Br−Ta−N(5)	97.85(11)
Ta−N(5)	1.753(3)	N(1)−Ta−N(2)	60.23(11)
N(1)−C(1)	1.338(5)	N(1)−Ta−N(3)	91.21(12)
N(2)−C(1)	1.337(4)	N(1)−Ta−N(4)	148.67(14)
N(3)−C(11)	1.356(5)	N(1)−Ta−N(5)	101.02(13)
N(4)−C(11)	1.426(5)	N(2)−Ta−N(3)	84.15(11)
N(5)−C(21)	1.438(4)	N(2)−Ta−N(4)	98.78(12)
		N(2)−Ta−N(5)	98.56(13)
		N(3)−Ta−N(4)	61.94(13)
		N(3)−Ta−N(5)	167.20(14)
		N(4)−Ta−N(5)	105.26(16)
		Ta−N(5)−C(21)	170.3(3)
		N(1)−C(1)−N(2)	111.1(3)
		N(3)−C(11)−N(4)	111.6(3)

The molecular structures of **9** and **10** are very similar. Each has distorted octahedral geometry about the tantalum centers, with one *tert*-butylimido ligand, two η^2-di-*tert*-butylacetamidinate ligands, and either a fluoride (**9**) or bromide (**10**) ligand. The tantalum-imido nitrogen bond lengths are 1.797(2) and 1.753(3) Å for **9** and **10**, respectively. The geometry about the imido nitrogen atom is approximately linear in each complex, with tantalum−nitrogen−carbon angles of 170.1(2)° in **9** and 170.3(3)° in **10**. The tantalum−nitrogen bond lengths for the amidinate ligands range from 2.100(3) to 2.362(3) Å (average = 2.22(11) Å) in **9**, with the longest bond being approximately *trans* to the imido nitrogen atom. Similarly, in **10** the tantalum−nitrogen bond lengths for the amidinate ligands range from 2.074(3) to 2.370(3) Å (average = 2.21(12) Å), with the longest bond lying approximately *trans* to the imido nitrogen atom. The amidinate ligand nitrogen−tantalum−nitrogen bite angles are 59.74(8)° and 60.09(10)° in **9**, and 60.23(11)° and 61.94(13)° in **10**. The carbon−nitrogen bonds in the amidinate ligand backbones vary between 1.331(3) and 1.375(4) Å in **9** and between 1.337(4) and 1.426(5) Å in **10**. Complex **9** contains a tantalum−fluorine bond of length 1.9434(16) Å, whereas **10** has a tantalum−bromine bond of length 2.565(2) Å. These bonds are *cis* to the imido linkages, with halide−tantalum−nitrogen bond angles of 101.27(9)° in **9** and 97.85(11)° in **10**.

Discussion

A central finding in the present work is the good volatility and high thermal stability of **3**, **4**, and **6**−**8**. These complexes begin to sublime between 120 and 150 °C/0.05 Torr, undergo preparative sublimations (0.5−1.0 g) with low residues between 150 and 175 °C/0.05 Torr, and decompose in the solid state between 297 and 340 °C. Complex **3** has the lowest sublimation temperature and highest decomposition temperature among this series. A preparative sublimation (0.7 g) using presublimed material afforded an 88% recovery of **3** after 4 h at 154 °C/0.05 Torr, with a nonvolatile residue of 0.4%. It was not possible to conduct a thermogravimetric analysis, since it would require a brief exposure to ambient atmosphere, and the extreme air sensitivity of **3** would lead to an artificially high nonvolatile residue. However, the high sublimed recovery, low nonvolatile residue, and high solid state decomposition temperature support the high thermal stability of **3**. The precursors $Ta(OEt)_5$,[16] $Ta(NMe_2)_5$,[17] and $Ta(NtBu)(NEt_2)_3$[18] show evidence for thermal decomposition in ALD growth at temperatures of $\leq$275 °C. Lower thermal decomposition temperatures in the solid or liquid states have been reported for $Ta(NMe_2)_5$ (180 °C),[30] $Ta(NtBu)(NMeEt)_3$ (185 °C),[25] and $Ta(NtBu)(NEt_2)_3$ (183 °C).[25] As such, the decomposition temperature of **3** is 65−90 °C higher and perhaps as much as 155−160 °C higher than these widely used tantalum ALD precursors. We have previously observed that the upper temperature range of self-limited ALD growth corresponds closely to the solid state decomposition temperatures of several metalorganic ALD precursors.[31] As such, use of **3** as an ALD precursor may allow self-limited growth up to about 340 °C. The high air sensitivity of **3** also suggests that it should react rapidly with water and other oxygen sources in ALD growth. ALD growth using **3** will be reported separately.[32] Fischer and co-workers have reported that closely related imido/amide/guanidinate complexes of the formula $Ta(NR^1)(R^2NC(NR^3R^4)NR^2)_2(NR^3R^4)$ (R^1−R^4 = alkyl) melt with decomposition in the solid state in the range of 195 to 232 °C.[25,26] Thus, **3** and the related amidinate complexes described herein are substantially more thermally stable than the structurally similar guanidinate analogues.

Chart 1. Proposed Transition State Structure for Ligand Exchange Processes in **2**, **9**, and **10**

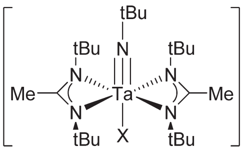

The broad resonances in the ^1H NMR spectra of **1**, **2**, **9**, and **10** at various temperatures demonstrate that ligand rearrangement processes are operant. Since the *tert*-butylimido resonance remains sharp in each case, while the amidinate resonances all broaden, the rearrangements must occur such that the four alkyl groups attached to the nitrogen atoms each end up in a different position. Also, the two methyl groups on the amidinate ligand backbone exchange positions. A possible mechanism for amidinate ligand rearrangement involves dissociation of the halide ligand, followed by amidinate ligand rearrangement through a square pyramidal intermediate, followed by halide ligand recoordination. Several factors, however, argue against this mechanism. ^1H NMR spectra of **1** and **9** in CD_2Cl_2 at 23 °C with ~5 equiv of PPN^+Cl^- (PPN^+ = bis(triphenylphosphoranylidene)ammonium) added showed no difference from those taken without PPN^+Cl^-. If chloride dissociation occurs in **1**, the presence of 5 equiv of chloride ion in solution would favor faster recombination with the tantalum complex, thus reducing the likelihood of rearrangement and therefore sharpening the peaks in the NMR spectrum. If fluoride dissociation occurs in **9**, the presence of 5 equiv of chloride in solution would favor at least some recombination of chloride with the cationic tantalum complex, forming **2** (not observed). Additionally, the $\Delta S^{\ddagger}$ values for **2**, **9**, and **10** are approximately −20 cal/mol·K for each complex. The negative $\Delta S^{\ddagger}$ values indicate more ordered transition states relative to the ground state and not the less ordered transition states that would result from halide ligand dissociation. To assess the possibility of bimolecular exchange, we determined the exchange rate constants for a solution of **2** in toluene-d_8 that had half the concentration of those used for the activation parameter data reported in Table 1. At any given temperature, the rate constant for this solution was the same within experimental error as the solution that was twice as concentrated. These data support a first order exchange process in **2**.

A reasonable transition state for ligand exchange in **2**, **9**, and **10** is shown in Chart 1. The transition state corresponds to a structure where the halide ligand occupies an axial site *trans* to the imido ligand, and the amidinate nitrogen atoms occupy equatorial sites. This structure is accessed by site exchange between the halide ligand and the amidinate nitrogen atom *trans* to the imido ligand nitrogen atom and contains two mirror planes that make the amidinate *tert*-butyl groups magnetically equivalent. Relaxation to the ground state structure then leads to amidinate *tert*-butyl group site exchange. The proposed transition state structure does not involve bond breaking and places the amidinate *tert*-butyl groups in more crowded positions than in the ground state structure. Hence, the transition state is more ordered than the ground state, consistent with the negative $\Delta S^{\ddagger}$ values. Complexes of the formula $Ta(NtBu)(iPrNC(NR_2)NiPr)_2(NR_2)$ (R = Me or Et) exhibit temperature dependent

---

[30] Bradley, D. C.; Thomas, I. M. *Can. J. Chem.* **1962**, *40*, 1355–1360.

[31] (a) Dezelah, C. L.IV; El-Kadri, O. M.; Szilágyi, I.; Campbell, J. M.; Arstila, K.; Niinistö, L.; Winter, C. H. *J. Am. Chem. Soc.* **2006**, *128*, 9638–9639. (b) Dezelah, C. L.IV; El-Kadri, O. M.; Kukli, K.; Arstila, K.; Baird, R. J.; Lu, J.; Niinistö, L.; Winter, C. H. *J. Mater. Chem.* **2007**, *17*, 1109–1116.

[32] Wiedmann, M. K.; Baird, R. J.; Winter, C. H., manuscript in preparation.

NMR spectra,[25] and may undergo dynamic processes similar to those of **2**, **9**, and **10**.

Many tantalum complexes containing amidinate or guanidinate ligands have been structurally characterized. These include complexes containing both imido and either amidinate or guanidinate ligands. The tantalum–nitrogen imido bond length of 1.797(2) in **9** is similar to those found in Ta(NPh)(PhNCHNPh)$_3$[27h] (1.801(9) Å), Ta(NPh)(PhNCHNPh)(PhNCHNHPh)Cl$_2$ (1.778(7) Å),[27k] and guanidinate complexes Ta(NR^1)(R^{2}NC(NR^{3}R^4)NR^2)$_2$(NR^{3}R^4) (1.78–1.80 Å).[25,26] The related bond length in **10** (1.753(3) Å) is slightly shorter. For comparison, the imido tantalum–nitrogen bond lengths are 1.737 and 1.70(2) Å in Ta(NtBu)(CH$_2$Ph)$_3$[27p] and [Ta(NtBu)(μ-OEt)Cl$_2$(NHtBu)]$_2$,[28b] respectively. The imido tantalum–nitrogen–carbon bond angles in **9** and **10** are 170.1(2)° and 170.3(3)°, respectively, which are close to linear. Since **9** and **10** are both d^0 and formally 14e$^-$ complexes, these angles are consistent with donation of the imido nitrogen atom lone pair to the tantalum center, creating a tantalum–nitrogen triple bond.

The tantalum–nitrogen amidinate ligand bond lengths in **9** and **10** vary greatly and range from 2.07 to 2.37 Å. The longest such bond length in each complex is *trans* to the imido group, owing to the strong *trans* influence of the latter, whereas the other tantalum–nitrogen bond length of the same amidinate ligand is the shortest in each complex. A similar trend is seen in other complexes. In Ta(NR^1)(R^{2}NC(NR^{3}R^4)NR^2)$_2$(NR^{3}R^4),[25,26] the tantalum–nitrogen bonds *trans* to the imido group range from 2.40 to 2.44 Å, whereas the other tantalum–nitrogen bonds in the same ligand fall between 2.12 and 2.14 Å. The tantalum–nitrogen bond lengths of the second guanidinate ligand in each complex are between 2.17 and 2.28 Å. In Ta(NPh)(PhNCHNPh)$_3$,[27h] the tantalum–nitrogen bond length *trans* to the imido group is 2.335(8) Å, whereas the other tantalum–nitrogen bond length in the same ligand is 2.188(8) Å. The tantalum–nitrogen bond lengths of the other two amidinate ligands range from 2.22 to 2.24 Å. Also in Ta(NPh)(PhNCHNPh)(PhNCHNHPh)Cl$_2$,[27k] the tantalum–nitrogen bond length *trans* to the imido nitrogen is 2.351(7) Å, whereas the other tantalum–nitrogen bond length in the same ligand is 2.123(8) Å. In other tantalum amidinate complexes lacking ligands with a large *trans* influence, the difference in Ta–N bond lengths is usually not more than about 0.1 Å.[27]

Crystals of **1**–**10** were grown from hexane and/or by sublimation, but only those of **9** and **10** gave crystal structures suitable for publication. Although several data sets on crystals of different batches of **2** were collected, in which the molecule could be seen, they all suffered from disorder and/or twinning. Crystals of the other compounds were even poorer in quality. Twinning is problematic in this series of complexes, especially in crystals grown by sublimation. The related imido/amide/guanidinate tantalum compounds Ta(NR^1)(R^{2}NC(NR^{3}R^4)NR^2)$_2$(NR^{3}R^4) suffer from a similar problem and were reported to form small, odd shaped crystallites that seemed to be twins or polymorphs.[25] Thermogravimetric and differential thermal analysis experiments indicated that solid-state reactions, most likely recrystallization processes, occur well below the melting points of the compounds. The presence of different phases was cited as a likely cause of the difficulty in obtaining crystals that were suitable for X-ray analysis. Also, Ta(iPrNCMeNiPr)$_2$Cl$_3$ crystallized as two different polymorphs under different conditions.[27a,27e]

Conclusions

A series of tantalum complexes containing *tert*-butylimido, two amidinate, and either a halide or a dialkylamide ligand has been synthesized. In each complex, the coordination sphere exhibits distorted octahedral geometry, with the imido and halide or dialkylamide ligands occupying coordination sites *cis* to each other. The less bulky complexes undergo ligand rearrangement in solution below 100 °C, and the kinetics of these processes was studied by variable temperature NMR. The negative entropies of activation indicate that the rearrangements occur by intramolecular processes with more ordered transition states rather than by dissociative processes. All of the complexes are volatile and sublime at low temperatures under reduced pressure. The dialkylamide complexes possess the highest thermal stabilities, and **3** has the lowest sublimation temperature and highest thermal stability among the series. Importantly, **3** undergoes thermal decomposition at 65–160 °C higher than widely used CVD and ALD precursors for tantalum, suggesting that this compound may be a very useful film growth precursor.

Experimental Section

General Considerations. All reactions were performed under argon using either glovebox or Schlenk line techniques. Tetrahydrofuran was distilled from sodium benzophenone ketyl, toluene was distilled from sodium, hexane was distilled from P$_2$O$_5$, and dichloromethane was distilled from CaH$_2$. Li(iPrNCMeNiPr) and Li(tBuNCMeNtBu) were prepared by treatment of *N*,*N*′-diisopropylcarbodiimide or *N*,*N*′-di-*tert*-butylcarbodiimide, respectively, with methyllithium.[33] Lithium ethyl methylamide[34] and Ta(NtBu)Cl$_3$(py)$_2$[35] were prepared according to literature procedures.

^{1}H and ^{13}C{^{1}H} NMR spectra were obtained at 500, 400, 300, 125, 100, or 75 MHz in toluene-d_8 or benzene-d_6 and were referenced to the residual proton and the ^{13}C resonances of the solvents. ^{19}F NMR spectra were obtained at 376 MHz and were referenced to external CFCl$_3$. Infrared spectra were obtained using Nujol as the medium. Elemental analyses were performed by Midwest Microlab, Indianapolis, IN. Melting points and thermal decomposition ranges were obtained on a Haake-Buchler HBI digital melting point apparatus and are uncorrected.

Preparation of Ta(NtBu)(iPrNCMeNiPr)$_2$Cl (1). A 100 mL Schlenk flask was charged with Ta(NtBu)Cl$_3$(py)$_2$ (1.998 g, 3.867 mmol), Li(iPrNCMeNiPr) (1.159 g, 7.822 mmol), and a stir bar. Toluene (80 mL) was added, and the yellow-orange mixture was stirred at ambient temperature for 24 h. The volatile components were then removed under reduced pressure to leave an orange paste. Hexane (40 mL) was added, and the mixture was filtered through a 2 cm pad of Celite on a coarse glass frit to yield an orange filtrate, which upon evaporation under reduced pressure gave **1** as a yellow solid (1.650 g, 75%). Recrystallization from hexane at −25 °C yielded yellow crystals of **1** (1.383 g, 63%): dec range 161–206 °C; IR (Nujol, cm^{-1}) 1620 (w), 1583 (s), 1509 (m), 1361 (m), 1351 (m), 1321 (m), 1276 (s), 1226 (m), 1211 (s), 1178 (m), 1144 (m), 1128 (m), 1059 (w), 1015 (w), 966 (w), 925 (m), 835 (m), 809 (m), 752 (w), 620 (w), 568 (w), 550 (w); ^{1}H NMR (300 MHz, toluene-d_8, −38 °C, δ) 3.77

---

(33) (a) Coles, M. P.; Swenson, D. C.; Jordan, R. F.; Young, V. G.Jr. *Organometallics* **1997**, *16*, 5183–5194. (b) Simpson, R. D.; Marshall, W. J. *Organometallics* **1997**, *16*, 3719–3722.

(34) Stubbert, B. D.; Stern, C. L.; Marks, T. J. *Organometallics* **2003**, *22*, 4836–4838.

(35) Chiu, H.-T.; Chuang, S.-H.; Tsai, C.-E.; Lee, G.-H; Peng, S.-M. *Polyhedron* **1998**, *17*, 2187–2190.

(septet, J = 6.5 Hz, 1H, C*H*), 3.74 (septet, J = 6.6 Hz, 1H, C*H*), 3.58 (septet, J = 6.4 Hz, 1H, C*H*), 3.47 (septet, J = 6.5 Hz, 1H, C*H*), 1.53 (m, 15H, C(C*H*$_3$)$_3$ overlapping with two CH-C*H*$_3$), 1.48 (d, J = 6.6 Hz, 6H, two overlapping CH-C*H*$_3$), 1.36 (d, J = 6.6 Hz, 3H, CH-C*H*$_3$), 1.33 (s, 6H, C−C*H*$_3$), 1.25 (d, J = 6.3 Hz, 3H, CH-C*H*$_3$), 1.02 (d, J = 6.6 Hz, 3H, CH-C*H*$_3$), 0.88 (d, J = 6.3 Hz, 3H, CH-C*H*$_3$); ^{13}C{^{1}H} NMR (75 MHz, toluene-*d*$_8$, −38 °C, ppm) 171.12 (s, *C*-CH$_3$), 168.32 (s, *C*-CH$_3$), 64.04 (s, *C*(CH$_3$)$_3$), 48.78 (s, *C*H), 48.55 (s, *C*H), 48.31 (s, *C*H), 47.07 (s, *C*H), 33.92 (s, C(*C*H$_3$)$_3$), 27.14 (s, CH-*C*H$_3$), 26.31 (s, CH-*C*H$_3$), 25.93 (s, CH-*C*H$_3$), 25.14 (s, CH-*C*H$_3$), 24.83 (s, two overlapping CH-*C*H$_3$), 23.20 (s, CH-*C*H$_3$), 22.62 (s, CH-*C*H$_3$), 10.60 (s, C-*C*H$_3$), 9.69 (s, C-*C*H$_3$). Anal. Calcd for $C_{20}H_{43}ClN_5Ta$: C, 42.14; H, 7.60; N, 12.29. Found: C, 42.41; H, 7.44; N, 12.41.

Preparation of Ta(NtBu)(tBuNCMeNtBu)$_2$Cl (2). In a fashion similar to the preparation of **1**, Ta(NtBu)Cl$_3$(py)$_2$ (1.500 g, 2.903 mmol) was treated with Li(tBuNCMeNtBu) (1.020 g, 5.788 mmol) to afford **2** as a yellow-brown solid (1.726 g, 95%). Recrystallization from hexane at −25 °C yielded crystals of **2** in the form of large yellow plates. Two more crops of crystals were grown from the concentrated mother liquor (1.112 g, 61%): dec range 260−270 °C; IR (Nujol, cm^{-1}) 1562 (m), 1556 (m), 1410 (w), 1311 (m), 1270 (m), 1232 (m), 1211 (m), 1195 (s), 1085 (m), 1038 (w), 997 (w), 825 (w), 795 (m); ^{1}H NMR (400 MHz, benzene-*d*$_6$, 23 °C, δ) 1.85 (s, 3H, C−C*H*$_3$), 1.82 (s, 3H, C−C*H*$_3$), 1.52 (s, 9H, C(C*H*$_3$)$_3$), 1.50 (s, 9H, C(C*H*$_3$)$_3$), 1.47 (s, 9H, imido C(C*H*$_3$)$_3$), 1.35 (s, 9H, C(C*H*$_3$)$_3$), 1.24 (s, 9H, C(C*H*$_3$)$_3$); ^{13}C{^{1}H} NMR (100 MHz, benzene-*d*$_6$, 23 °C, ppm) 173.44 (s, *C*-CH$_3$), 170.28 (s, *C*-CH$_3$), 64.15 (s, imido *C*(CH$_3$)$_3$), 54.26 (s, *C*(CH$_3$)$_3$), 53.97 (s, *C*(CH$_3$)$_3$), 53.44 (s, *C*(CH$_3$)$_3$), 52.41 (s, *C*(CH$_3$)$_3$), 34.09 (s, C(*C*H$_3$)$_3$), 33.78 (s, C(*C*H$_3$)$_3$), 33.69 (s, C(*C*H$_3$)$_3$), 32.98 (s, C(*C*H$_3$)$_3$), 32.27 (s, C(*C*H$_3$)$_3$), 21.69 (s, C-*C*H$_3$), 20.92 (s, C-*C*H$_3$). Anal. Calcd for $C_{24}H_{51}ClN_5Ta$: C, 46.04; H, 8.21; N, 11.19. Found: C, 46.30; H, 8.18; N, 11.12.

Preparation of Ta(NtBu)(iPrNCMeNiPr)$_2$(NMe$_2$) (3). A 100 mL Schlenk flask was charged with **1** (1.062 g, 1.863 mmol), LiNMe$_2$ (0.141 g, 2.76 mmol), and a stir bar. Tetrahydrofuran (40 mL) was added, and the yellow solution was stirred at ambient temperature for 18 h, after which time the volatile components were removed under reduced pressure, leaving a yellow solid. Hexane (25 mL) was added, and the mixture was filtered through a 2 cm pad of Celite on a coarse glass frit. The solvent was removed from the pale yellow filtrate under reduced pressure, giving **3** as a pale yellow solid (0.954 g, 89%). The crude product was sublimed at 155 °C/0.05 Torr to afford **3** as white crystals (0.719 g, 67%): dec range 324−340 °C; IR (Nujol, cm^{-1}) 2808 (m), 2762 (m), 2602 (w), 1531 (s), 1421 (m), 1411 (m), 1359 (m), 1346 (s), 1314 (m), 1271 (s), 1242 (w), 1222 (s), 1207 (s), 1176 (m), 1145 (m), 1125 (w), 1057 (w), 1045 (w), 1015 (m), 971 (s), 830 (w), 810 (m), 625 (w), 574 (w), 549 (w); ^{1}H NMR (400 MHz, benzene-*d*$_6$, 23 °C, δ) 4.14 (s, 3H, NC*H*$_3$), 3.79 (septet, J = 6.1 Hz, 1H, C*H*), 3.74 (septet, J = 6.1 Hz, 1H, C*H*), 3.57 (septet, J = 6.3 Hz, 1H, C*H*), 3.46 (s, 3H, NC*H*$_3$), 3.40 (septet, J = 6.5 Hz, 1H, C*H*), 1.49 (m, 18H, overlapping C(C*H*$_3$)$_3$ and CH-C*H*$_3$ and two C−C*H*$_3$), 1.37 (d, J = 6.4 Hz, 3H, CH-C*H*$_3$), 1.32 (d, J = 5.6 Hz, 3H, CH-C*H*$_3$), 1.26 (d, J = 6.8 Hz, 3H, CH-C*H*$_3$), 1.18 (d, J = 6.8 Hz, 3H, CH-C*H*$_3$), 1.12 (d, J = 6.4 Hz, 3H, CH-C*H*$_3$), 1.07 (d, J = 6.4 Hz, 3H, CH-C*H*$_3$), 0.94 (d, J = 6.4 Hz, 3H, CH-C*H*$_3$); ^{13}C{^{1}H} NMR (100 MHz, benzene-*d*$_6$, 23 °C, ppm) 171.69 (s, *C*-CH$_3$), 168.76 (s, *C*-CH$_3$), 63.53 (s, *C*(CH$_3$)$_3$), 57.90 (s, N*C*H$_3$), 48.52 (s, *C*H), 48.19 (s, *C*H), 47.91 (s, *C*H overlapping with N*C*H$_3$), 47.24 (s, *C*H), 34.82 (s, C(*C*H$_3$)$_3$), 26.76 (s, CH-*C*H$_3$), 25.87 (s, CH-*C*H$_3$), 25.77 (s, two overlapping CH-*C*H$_3$), 25.65 (s, two overlapping CH-*C*H$_3$), 24.03 (s, CH-*C*H$_3$), 23.82 (s, CH-*C*H$_3$), 12.39 (s, C-*C*H$_3$), 10.95 (s, C-*C*H$_3$). Anal. Calcd for $C_{22}H_{49}N_6Ta$: C, 45.67; H, 8.54; N, 14.53. Found: C, 45.48; H, 8.29; N, 14.25.

Preparation of Ta(NtBu)(tBuNCMeNtBu)$_2$(NMe$_2$) (4). In a fashion similar to the preparation of **3**, treatment of **2** (0.505 g, 0.806 mmol) with LiNMe$_2$ (0.080 g, 1.6 mmol) afforded **4** as a slightly off-white solid (0.438 g, 86%). Recrystallization from hexane at −25 °C yielded colorless needles of **4** (0.231 g, 45%): dec range 298−309 °C, IR (Nujol, cm^{-1}) 2761 (w), 1506 (w), 1406 (w), 1313 (w), 1264 (m), 1228 (m), 1210 (m), 1196 (s), 1080 (w), 1036 (w), 998 (w), 971 (s), 889 (w), 825 (w), 791 (w), 662 (w); ^{1}H NMR (400 MHz, benzene-*d*$_6$, 23 °C, δ) 4.10 (s, 3H, NC*H*$_3$), 3.40 (s, 3H, NC*H*$_3$), 1.88 (s, 3H, C−C*H*$_3$), 1.87 (s, 3H, C−C*H*$_3$), 1.48 (s, 18H, two overlapping C(C*H*$_3$)$_3$), 1.38 (s, 9H, C(C*H*$_3$)$_3$), 1.37 (s, 9H, C(C*H*$_3$)$_3$), 1.33 (s, 9H, C(C*H*$_3$)$_3$); ^{13}C{^{1}H} NMR (100 MHz, benzene-*d*$_6$, 23 °C, ppm) 173.51 (s, *C*-CH$_3$), 170.03 (s, *C*-CH$_3$), 63.67 (s, imido *C*(CH$_3$)$_3$), 58.49 (s, N*C*H$_3$), 53.74 (s, *C*(CH$_3$)$_3$), 52.44 (s, *C*(CH$_3$)$_3$), 52.16 (s, *C*(CH$_3$)$_3$), 51.91 (s, *C*(CH$_3$)$_3$), 48.05 (s, N*C*H$_3$), 34.87 (s, C(*C*H$_3$)$_3$), 34.55 (s, C(*C*H$_3$)$_3$), 33.41 (s, C(*C*H$_3$)$_3$), 33.33 (s, C(*C*H$_3$)$_3$), 32.93 (s, C(*C*H$_3$)$_3$), 22.34 (s, C-*C*H$_3$), 21.03 (s, C-*C*H$_3$). Anal. Calcd for $C_{26}H_{57}N_6Ta$: C, 49.20; H, 9.05; N, 13.24. Found: C, 48.72; H, 8.77; N, 12.96.

Preparation of Ta(NtBu)(iPrNCMeNiPr)$_2$(NEt$_2$) (5). In a fashion similar to the preparation of **3**, treatment of **1** (0.152 g, 0.267 mmol) with LiNEt$_2$ (0.032 g, 0.40 mmol) afforded **5** as a pale beige solid (0.138 g, 85%). The crude product was sublimed at 147 °C/0.05 Torr to afford **5** as colorless crystals (0.090 g, 56%): dec range 244−259 °C; IR (Nujol, cm^{-1}) 2604 (w), 1651 (w), 1622 (w), 1584 (m), 1533 (s), 1415 (s), 1350 (s), 1315 (s), 1270 (s), 1221 (s), 1208 (s), 1178 (s), 1144 (s), 1126 (m), 1091 (w), 1058 (m), 1045 (w), 1013 (s), 967 (w), 928 (w), 889 (m), 833 (w), 810 (m), 788 (m), 622 (m), 574 (w), 549 (w), 534 (w); ^{1}H NMR (400 MHz, benzene-*d*$_6$, 23 °C, δ) 4.69 (dq, J = 13.6, 6.8 Hz, 1H, NC*H*$_2$CH$_3$), 4.29 (m, 2H, two overlapping NC*H*$_2$CH$_3$), 3.79 (septet, J = 6.3 Hz, 1H, C*H*), 3.75 (septet, J = 6.3 Hz, 1H, C*H*), 3.59 (septet, J = 6.3 Hz, 1H, C*H*), 3.39 (septet, J = 6.5 Hz, 1H, C*H*), 3.22 (dq, J = 13.2, 6.6 Hz, 1H, NC*H*$_2$CH$_3$), 1.49 (m, 18H, overlapping C(C*H*$_3$)$_3$ and CH-C*H*$_3$ and two C−C*H*$_3$), 1.46 (t, J = 6.8 Hz, 3H, NCH$_2$C*H*$_3$), 1.40 (d, J = 6.4 Hz, 3H, CH-C*H*$_3$), 1.33 (d, J = 6.8 Hz, 3H, CH-C*H*$_3$), 1.27 (d, J = 6.4 Hz, 6H, two overlapping CH-C*H*$_3$), 1.08 (d, J = 6.4 Hz, 3H, CH-C*H*$_3$), 1.07 (d, J = 6.4 Hz, 3H, CH-C*H*$_3$), 0.97 (t, J = 7.0 Hz, 3H, NCH$_2$C*H*$_3$), 0.93 (d, J = 6.4 Hz, 3H, CH-C*H*$_3$); ^{13}C{^{1}H} NMR (75 MHz, benzene-*d*$_6$, 23 °C, ppm) 171.99 (s, *C*-CH$_3$), 168.69 (s, *C*-CH$_3$), 63.60 (s, *C*(CH$_3$)$_3$), 58.19 (s, N*C*H$_2$CH$_3$), 48.28 (s, *C*H), 48.19 (s, *C*H), 48.15 (s, *C*H), 47.71 (s, N*C*H$_2$CH$_3$), 47.27 (s, *C*H), 34.60 (s, C(*C*H$_3$)$_3$), 27.04 (s, CH-*C*H$_3$), 26.31 (s, CH-*C*H$_3$), 25.95 (s, CH-*C*H$_3$), 25.83 (s, two overlapping CH-*C*H$_3$), 24.77 (s, CH-*C*H$_3$), 24.11 (s, CH-*C*H$_3$), 23.53 (s, CH-*C*H$_3$), 17.76 (s, NCH$_2$*C*H$_3$), 15.79 (s, NCH$_2$*C*H$_3$), 12.50 (s, C-*C*H$_3$), 11.01 (s, C-*C*H$_3$). Anal. Calcd for $C_{24}H_{53}N_6Ta$: C, 47.51; H, 8.81; N, 13.85. Found: C, 47.61; H, 8.65; N, 13.75.

Preparation of Ta(NtBu)(tBuNCMeNtBu)$_2$(NEt$_2$) (6). In a fashion similar to the preparation of **3**, treatment of **2** (0.220 g, 0.351 mmol) with LiNEt$_2$ (0.078 g, 0.99 mmol) gave **6** as a light orange solid (0.184 g, 79%). The crude product was sublimed at 176 °C/0.05 Torr to yield **6** as colorless crystals (0.111 g, 48%): dec range 298−321 °C; IR (Nujol, cm^{-1}) 1506 (s), 1406 (m), 1366 (s), 1260 (s), 1228 (m), 1208 (m), 1193 (s), 1146 (m), 1078 (m), 1035 (m), 1014 (m), 996 (m), 889 (m), 880 (m), 825 (m), 788 (m), 662 (m), 610 (w), 577 (w); ^{1}H NMR (400 MHz, benzene-*d*$_6$, 23 °C, δ) 4.67 (dq, J = 13.0, 7.2 Hz, 1H, NC*H*$_2$CH$_3$), 4.36 (dq, J = 13.0, 7.2 Hz, 1H, NC*H*$_2$CH$_3$), 4.19 (dq, J = 12.8, 7.2 Hz, 1H, NC*H*$_2$CH$_3$), 3.30 (dq, J = 13.0, 6.7 Hz, 1H, NC*H*$_2$CH$_3$), 1.89 (s, C−C*H*$_3$), 1.88 (s, C−C*H*$_3$), 1.52 (s, 9H, C(C*H*$_3$)$_3$), 1.47 (s, 9H, C(C*H*$_3$)$_3$), 1.42 (t, J = 7.0 Hz, 3H, NCH$_2$C*H*$_3$), 1.41 (s, 9H, C(C*H*$_3$)$_3$), 1.38 (s, 9H, C(C*H*$_3$)$_3$), 1.32 (s, 9H, C(C*H*$_3$)$_3$), 1.01 (t, J = 7.2 Hz, 3H, NCH$_2$C*H*$_3$); ^{13}C{^{1}H} NMR (125 MHz, benzene-*d*$_6$, 23 °C, ppm) 173.54 (s, *C*-CH$_3$), 170.26 (s, *C*-CH$_3$), 63.80 (s, imido *C*(CH$_3$)$_3$), 59.42

(s, $\mathrm{N}C\mathrm{H_2CH_3}$), 53.15 (s, $C\mathrm{(CH_3)_3}$), 52.39 (s, $C\mathrm{(CH_3)_3}$), 51.92 (s, two overlapping $C\mathrm{(CH_3)_3}$), 48.85 (s, $\mathrm{N}C\mathrm{H_2CH_3}$), 34.62 (s, $\mathrm{C(}C\mathrm{H_3)_3}$), 34.57 (s, $\mathrm{C(}C\mathrm{H_3)_3}$), 33.58 (s, $\mathrm{C(}C\mathrm{H_3)_3}$), 33.40 (s, $\mathrm{C(}C\mathrm{H_3)_3}$), 33.32 (s, $\mathrm{C(}C\mathrm{H_3)_3}$), 22.12 (s, $\mathrm{C\text{-}}C\mathrm{H_3}$), 21.33 (s, $\mathrm{C\text{-}}C\mathrm{H_3}$), 17.64 (s, $\mathrm{NCH_2}C\mathrm{H_3}$), 15.97 (s, $\mathrm{NCH_2}C\mathrm{H_3}$). Anal. Calcd for $\mathrm{C_{28}H_{61}N_6Ta}$: C, 50.74; H, 9.28; N, 12.68. Found: C, 50.18; H, 9.02; N, 12.39.

Preparation of Ta(NtBu)(iPrNCMeNiPr)$_2$(NEtMe) (7). In a fashion similar to the preparation of **3**, treatment of **1** (2.672 g, 4.688 mmol) with LiNEtMe (0.335 g, 5.15 mmol) gave **7** as a gold-colored solid (2.567 g, 92%). The crude product was sublimed at 160 °C/0.05 Torr to yield **7** as cream-colored crystals (2.423 g, 87%): dec range 300−322 °C; IR (Nujol, cm^{-1}) 1533 (s), 1415 (w), 1348 (m), 1314 (w), 1269 (s), 1222 (m), 1207 (s), 1176 (m), 1147 (m), 1125 (w), 1079 (w), 1057 (w), 1046 (w), 1014 (w), 997 (m), 935 (w), 885 (m), 832 (w), 810 (m), 625 (w), 579 (w); ^{1}H NMR (500 MHz, benzene-d_6, 23 °C, δ) major isomer: 4.48 (dq, J = 12.3, 7.0 Hz, 1H, $\mathrm{NC}H_2\mathrm{CH_3}$), 4.18 (s, 3H, $\mathrm{NC}H_3$), 3.78 (septet, J = 6.5 Hz, 1H, $\mathrm{C}H$), 3.74 (septet, J = 6.5 Hz, 1H, $\mathrm{C}H$), 3.57 (septet, J = 6.5 Hz, 1H, $\mathrm{C}H$), 3.37 (septet, J = 6.5 Hz, 1H, $\mathrm{C}H$), 2.91 (dq, J = 13.0, 6.5 Hz, 1H, $\mathrm{NC}H_2\mathrm{CH_3}$), 1.49 (m, 18H, overlapping $\mathrm{C(C}H_3\mathrm{)_3}$ and $\mathrm{CH\text{-}C}H_3$ and two $\mathrm{C{-}C}H_3$), 1.40 (d, J = 6.5 Hz, 3H, $\mathrm{CH\text{-}C}H_3$), 1.34 (d, J = 7.0 Hz, 3H, $\mathrm{CH\text{-}C}H_3$), 1.26 (d, J = 6.0 Hz, 3H, $\mathrm{CH\text{-}C}H_3$), 1.18 (d, J = 6.5 Hz, 3H, $\mathrm{CH\text{-}C}H_3$), 1.09 (d, J = 7.0 Hz, 3H, $\mathrm{CH\text{-}C}H_3$), 1.07 (d, J = 6.5 Hz, 3H, $\mathrm{CH\text{-}C}H_3$), 0.97 (t, J = 7.0 Hz, 3H, $\mathrm{NCH_2C}H_3$), 0.92 (d, J = 6.5 Hz, 3H, $\mathrm{CH\text{-}C}H_3$), minor isomer: 4.75 (dq, J = 12.0, 7.5 Hz, 1H, $\mathrm{NC}H_2\mathrm{CH_3}$), 4.15 (dq, J = 12.5, 7.0 Hz, 1H, $\mathrm{NC}H_2\mathrm{CH_3}$), 3.80 (septet, J = 6.5 Hz, 1H, $\mathrm{C}H$), 3.75 (septet, J = 6.5 Hz, 1H, $\mathrm{C}H$), 3.58 (septet, J = 6.5 Hz, 1H, $\mathrm{C}H$), 3.46 (s, 3H, $\mathrm{NC}H_3$), 3.41 (septet, J = 6.5 Hz, 1H, $\mathrm{C}H$), 1.49 (m, 18H, overlapping $\mathrm{C(C}H_3\mathrm{)_3}$ and $\mathrm{CH\text{-}C}H_3$ and two $\mathrm{C{-}C}H_3$), 1.39 (d, J = 6.5 Hz, 3H, $\mathrm{CH\text{-}C}H_3$), 1.37 (t, J = 7.0 Hz, 3H, $\mathrm{NCH_2C}H_3$), 1.33 (d, J = 6.5 Hz, 3H, $\mathrm{CH\text{-}C}H_3$), 1.26 (d, J = 6.0 Hz, 3H, $\mathrm{CH\text{-}C}H_3$), 1.22 (d, J = 6.5 Hz, 3H, $\mathrm{CH\text{-}C}H_3$), 1.13 (d, J = 6.5 Hz, 3H, $\mathrm{CH\text{-}C}H_3$), 1.08 (d, J = 6.0 Hz, 3H, $\mathrm{CH\text{-}C}H_3$), 0.93 (d, J = 6.5 Hz, 3H, $\mathrm{CH\text{-}C}H_3$); $^{13}\mathrm{C}\{^1\mathrm{H}\}$ NMR (125 MHz, benzene-d_6, 23 °C, ppm) major isomer: 171.76 (s, $C\mathrm{\text{-}CH_3}$), 168.90 (s, $C\mathrm{\text{-}CH_3}$), 63.55 (s, $C\mathrm{(CH_3)_3}$), 53.82 (s, $\mathrm{N}C\mathrm{H_3}$), 52.91 (s, $\mathrm{N}C\mathrm{H_2CH_3}$), 48.49 (s, $C\mathrm{H}$), 48.21 (s, $C\mathrm{H}$), 48.11 (s, $C\mathrm{H}$), 47.27 (s, $C\mathrm{H}$), 34.81 (s, $\mathrm{C(}C\mathrm{H_3)_3}$), 27.21 (s, $\mathrm{CH\text{-}}C\mathrm{H_3}$), 25.94 (s, $\mathrm{CH\text{-}}C\mathrm{H_3}$), 25.91 (s, $\mathrm{CH\text{-}}C\mathrm{H_3}$), 25.89 (s, $\mathrm{CH\text{-}}C\mathrm{H_3}$), 25.77 (s, two overlapping $\mathrm{CH\text{-}}C\mathrm{H_3}$), 23.99 (s, $\mathrm{CH\text{-}}C\mathrm{H_3}$), 23.57 (s, $\mathrm{CH\text{-}}C\mathrm{H_3}$), 14.57 (s, $\mathrm{NCH_2}C\mathrm{H_3}$), 12.38 (s, $\mathrm{C\text{-}}C\mathrm{H_3}$), 10.83 (s, $\mathrm{C\text{-}}C\mathrm{H_3}$), minor isomer: 171.65 (s, $C\mathrm{\text{-}CH_3}$), 168.78 (s, $C\mathrm{\text{-}CH_3}$), 63.82 (s, $\mathrm{N}C\mathrm{H_2CH_3}$), 63.55 (imido $C\mathrm{(CH_3)_3}$ obscured by major isomer), 48.44 (s, $C\mathrm{H}$), 47.93 (s, $C\mathrm{H}$), 48.9−47.9 (two $C\mathrm{H}$ obscured), 43.50 (s, $\mathrm{N}C\mathrm{H_3}$), 34.68 (s, $\mathrm{C(}C\mathrm{H_3)_3}$), 26.85 (s, $\mathrm{CH\text{-}}C\mathrm{H_3}$), 26.14 (s, $\mathrm{CH\text{-}}C\mathrm{H_3}$), 26.01 (s, $\mathrm{CH\text{-}}C\mathrm{H_3}$), 25.82 (s, $\mathrm{CH\text{-}}C\mathrm{H_3}$), 25.63 (s, $\mathrm{CH\text{-}}C\mathrm{H_3}$), 25.30 (s, $\mathrm{CH\text{-}}C\mathrm{H_3}$), 24.04 (s, $\mathrm{CH\text{-}}C\mathrm{H_3}$), 23.71 (s, $\mathrm{CH\text{-}}C\mathrm{H_3}$), 15.93 (s, $\mathrm{NCH_2}C\mathrm{H_3}$), 12.57 (s, $\mathrm{C\text{-}}C\mathrm{H_3}$), 11.05 (s, $\mathrm{C\text{-}}C\mathrm{H_3}$). Anal. Calcd for $\mathrm{C_{23}H_{51}N_6Ta}$: C, 46.61; H, 8.67; N, 14.18. Found: C, 46.63; H, 8.60; N, 14.28.

Preparation of Ta(NtBu)(tBuNCMeNtBu)$_2$(NEtMe) (8). In a fashion similar to the preparation of **3**, treatment of **2** (0.404 g, 0.645 mmol) with LiNEtMe (0.048 g, 0.74 mmol) gave **8** as a yellow solid (0.347 g, 83%). Sublimation of 0.288 g of crude product at 170 °C/0.05 Torr yielded **8** as pale yellow crystals (0.234 g, 81% recovery): dec range 297−306 °C; IR (Nujol, cm^{-1}) 1501 (w), 1465 (s), 1408 (w), 1306 (w), 1263 (s), 1229 (m), 1209 (w), 1196 (m), 1170 (w), 1148 (w), 1079 (m), 1035 (m), 998 (m), 966 (w), 935 (w), 889 (w), 846 (w), 824 (w), 791 (m), 771 (w), 662 (w); ^{1}H NMR (500 MHz, benzene-d_6, 23 °C, δ) major isomer: 4.35 (dq, J = 12.0, 7.0 Hz, 1H, $\mathrm{NC}H_2\mathrm{CH_3}$), 4.12 (s, 3H, $\mathrm{NC}H_3$), 2.87 (dq, J = 12.5, 6.8 Hz, 1H, $\mathrm{NC}H_2\mathrm{CH_3}$), 1.88 (s, 3H, $\mathrm{C{-}C}H_3$), 1.87 (s, 3H, $\mathrm{C{-}C}H_3$), 1.51 (s, 9H, $\mathrm{C(C}H_3\mathrm{)_3}$), 1.48 (s, 9H, $\mathrm{C(C}H_3\mathrm{)_3}$), 1.39 (s, 9H, $\mathrm{C(C}H_3\mathrm{)_3}$), 1.38 (s, 9H, $\mathrm{C(C}H_3\mathrm{)_3}$), 1.32 (s, 9H, $\mathrm{C(C}H_3\mathrm{)_3}$), 0.98 (t, J = 7.0 Hz, 3H, $\mathrm{NCH_2C}H_3$), minor isomer: 5.01 (dq, J = 12.5, 7.3 Hz, 1H, $\mathrm{NC}H_2\mathrm{CH_3}$), 3.76 (dq, J = 12.5, 7.0 Hz, 1H, $\mathrm{NC}H_2\mathrm{CH_3}$), 3.40 (s, 3H, $\mathrm{NC}H_3$), 1.89 (s, 3H, $\mathrm{C{-}C}H_3$), 1.88 (s, 3H, $\mathrm{C{-}C}H_3$), 1.51 (s, 9H, $\mathrm{C(C}H_3\mathrm{)_3}$), 1.47 (s, 9H, $\mathrm{C(C}H_3\mathrm{)_3}$), 1.39 (s, 9H, $\mathrm{C(C}H_3\mathrm{)_3}$), 1.38 (s, 9H, $\mathrm{C(C}H_3\mathrm{)_3}$), 1.36 (t, J = 7.0 Hz, 3H, $\mathrm{NCH_2C}H_3$), 1.33 (s, 9H, $\mathrm{C(C}H_3\mathrm{)_3}$); $^{13}\mathrm{C}\{^1\mathrm{H}\}$ NMR (125 MHz, benzene-d_6, 23 °C, ppm) major isomer: 173.40 (s, $C\mathrm{\text{-}CH_3}$), 170.45 (s, $C\mathrm{\text{-}CH_3}$), 63.71 (s, imido $C\mathrm{(CH_3)_3}$), 53.81 (s, $\mathrm{N}C\mathrm{H_3}$), 53.74 (s, $C\mathrm{(CH_3)_3}$), 53.14 (s, $\mathrm{N}C\mathrm{H_2CH_3}$), 52.34 (s, $C\mathrm{(CH_3)_3}$), 52.14 (s, $C\mathrm{(CH_3)_3}$), 51.93 (s, $C\mathrm{(CH_3)_3}$), 34.86 (s, $\mathrm{C(}C\mathrm{H_3)_3}$), 34.72 (s, $\mathrm{C(}C\mathrm{H_3)_3}$), 33.49 (s, $\mathrm{C(}C\mathrm{H_3)_3}$), 33.22 (s, $\mathrm{C(}C\mathrm{H_3)_3}$), 33.18 (s, $\mathrm{C(}C\mathrm{H_3)_3}$), 22.13 (s, $\mathrm{C\text{-}}C\mathrm{H_3}$), 21.22 (s, $\mathrm{C\text{-}}C\mathrm{H_3}$), 14.31 (s, $\mathrm{NCH_2}C\mathrm{H_3}$), minor isomer: 173.60 (s, $C\mathrm{\text{-}CH_3}$), 170.18 (s, $C\mathrm{\text{-}CH_3}$), 64.90 (s, $\mathrm{N}C\mathrm{H_2CH_3}$), 63.71 (imido $C\mathrm{(CH_3)_3}$ obscured by major isomer), 53.62 (s, $C\mathrm{(CH_3)_3}$), 52.20 (s, $C\mathrm{(CH_3)_3}$), 52.02 (s, $C\mathrm{(CH_3)_3}$), 51.89 (s, $C\mathrm{(CH_3)_3}$), 43.67 (s, $\mathrm{N}C\mathrm{H_3}$), 34.74 (s, $\mathrm{C(}C\mathrm{H_3)_3}$), 34.50 (s, $\mathrm{C(}C\mathrm{H_3)_3}$), 33.59 (s, $\mathrm{C(}C\mathrm{H_3)_3}$), 33.50 (s, $\mathrm{C(}C\mathrm{H_3)_3}$), 33.18 (s, $\mathrm{C(}C\mathrm{H_3)_3}$), 22.20 (s, $\mathrm{C\text{-}}C\mathrm{H_3}$), 21.13 (s, $\mathrm{C\text{-}}C\mathrm{H_3}$), 15.73 (s, $\mathrm{NCH_2}C\mathrm{H_3}$). Anal. Calcd for $\mathrm{C_{27}H_{59}N_6Ta}$: C, 49.99; H, 9.17; N, 12.95. Found: C, 50.11; H, 8.89; N, 12.71.

Preparation of Ta(NtBu)(tBuNCMeNtBu)$_2$F (9). A 100 mL Schlenk flask was charged with **2** (0.305 g, 0.487 mmol), $\mathrm{AgBF_4}$ (0.126 g, 0.647 mmol), and a stir bar. Dichloromethane (20 mL) was added, and the mixture was stirred at ambient temperature for 28 h. The volatile components were removed under reduced pressure, leaving a purple solid. Hexane (20 mL) was added, and the mixture filtered through a 2 cm pad of Celite on a coarse glass frit. Removal of the volatile components from the colorless filtrate under reduced pressure afforded **9** as a beige solid (0.160 g, 54%). Sublimation of the crude product at 146 °C/0.05 Torr yielded **9** as white crystals (0.111 g, 37%). Crystals suitable for X-ray diffraction were grown from hexane at −25 °C: mp 257−259 °C; IR (Nujol, cm^{-1}) 1544 (m), 1411 (w), 1325 (m), 1274 (m), 1231 (m), 1198 (s), 1102 (w), 1086 (m), 1037 (m), 998 (m), 891 (w), 833 (w), 822 (m), 792 (m), 662 (w), 558 (w); ^{1}H NMR (300 MHz, toluene-d_8, −64 °C, δ) 1.80 (s, 3H, $\mathrm{C{-}C}H_3$), 1.71 (s, 3H, $\mathrm{C{-}C}H_3$), 1.56 (s, 18H, two $\mathrm{C(C}H_3\mathrm{)_3}$), 1.52 (s, 9H, imido $\mathrm{C(C}H_3\mathrm{)_3}$), 1.33 (s, 9H, $\mathrm{C(C}H_3\mathrm{)_3}$), 1.31 (s, 9H, $\mathrm{C(C}H_3\mathrm{)_3}$); $^{13}\mathrm{C}\{^1\mathrm{H}\}$ NMR (75 MHz, toluene-d_8, −64 °C, ppm) 173.46 (s, $C\mathrm{\text{-}CH_3}$), 169.35 (s, $C\mathrm{\text{-}CH_3}$), 63.43 (s, imido $C\mathrm{(CH_3)_3}$), 53.83 (s, $C\mathrm{(CH_3)_3}$), 53.38 (s, $C\mathrm{(CH_3)_3}$), 53.15 (s, $C\mathrm{(CH_3)_3}$), 51.88 (s, $C\mathrm{(CH_3)_3}$), 34.50 (s, $\mathrm{C(}C\mathrm{H_3)_3}$), 33.85 (s, $\mathrm{C(}C\mathrm{H_3)_3}$), 32.55 (s, two $\mathrm{C(}C\mathrm{H_3)_3}$), 31.32 (s, $\mathrm{C(}C\mathrm{H_3)_3}$), 21.54 (s, $\mathrm{C\text{-}}C\mathrm{H_3}$), 20.07 (s, $\mathrm{C\text{-}}C\mathrm{H_3}$ obscured by toluene-d_8 peak); ^{19}F NMR (376 MHz, benzene-d_6, 23 °C, ppm) 10.06 (s, 1F). Anal. Calcd for $\mathrm{C_{24}H_{51}FN_5Ta}$: C, 47.28; H, 8.43; N, 11.49. Found: C, 47.16; H, 8.22; N, 11.32.

Preparation of Ta(NtBu)(tBuNCMeNtBu)$_2$Br (10). A 100 mL Schlenk flask was charged with **2** (0.319 g, 0.510 mmol), dichloromethane (20 mL) and a stir bar. While connected to a bubbler, $\mathrm{BBr_3}$ (1.0 M in $\mathrm{CH_2Cl_2}$, 0.26 mL, 0.26 mmol) was added to the solution. After 3 h the connection to the bubbler was removed, but the bright yellow solution was stirred further at ambient temperature, for a total of 20 h. The volatile components were then removed under reduced pressure, leaving a yellow solid. Hexane (20 mL) was added, and the mixture was filtered through a 2 cm pad of Celite on a coarse glass frit. The solvent was removed from the bright yellow filtrate under reduced pressure to afford **10** as a bright yellow solid (0.234 g, 68%). Recrystallization from hexane at −25 °C yielded **10** as bright yellow rods (0.173 g, 51%): dec range 213−228 °C; IR (Nujol, cm^{-1}) 1560 (m), 1408 (w), 1366 (m), 1307 (m), 1269 (m), 1228 (w), 1210 (w), 1194 (s), 1084 (m), 1038 (m), 995 (w), 883 (w), 825 (m), 795 (m), 772 (w), 662 (w); ^{1}H NMR (300 MHz, benzene-d_6, 23 °C, δ) 1.83 (s, 3H, $\mathrm{C{-}C}H_3$), 1.80 (s, 3H, $\mathrm{C{-}C}H_3$), 1.53 (s, 9H, $\mathrm{C(C}H_3\mathrm{)_3}$), 1.51 (s, 9H, $\mathrm{C(C}H_3\mathrm{)_3}$), 1.49 (s, 9H, imido $\mathrm{C(C}H_3\mathrm{)_3}$), 1.37 (s, 9H, $\mathrm{C(C}H_3\mathrm{)_3}$), 1.22 (s, 9H, $\mathrm{C(C}H_3\mathrm{)_3}$); $^{13}\mathrm{C}\{^1\mathrm{H}\}$ NMR (75 MHz, toluene-d_8, 23 °C, ppm) 173.47 (s, $C\mathrm{\text{-}CH_3}$), 170.37 (s, $C\mathrm{\text{-}CH_3}$), 64.37 (s, imido $C\mathrm{(CH_3)_3}$), 54.30 (s, two overlapping $C\mathrm{(CH_3)_3}$), 53.66 (s, $C\mathrm{(CH_3)_3}$), 52.54 (s, $C\mathrm{(CH_3)_3}$), 34.10 (s, C(CH_3)$_3$), 34.02 (s, C(CH_3)$_3$), 33.57 (s, C(CH_3)$_3$), 33.06 (s, C(CH_3)$_3$), 32.47 (s, C(CH_3)$_3$), 21.81 (s, C-CH_3), 21.10 (s, C-CH_3). Anal. Calcd for $C_{24}H_{51}BrN_5Ta$: C, 42.99; H, 7.67; N, 10.44. Found: C, 43.18; H, 7.49; N, 10.17.

Kinetics Study of Ligand Rearrangement. A typical sample was prepared by dissolving ~20 mg of the compound to be studied in ~0.85 mL toluene-d_8 in an NMR tube. ^{1}H NMR spectra were recorded at 300 MHz in the range of −64 to 104 °C. The temperatures were calibrated by running methanol (low temperature) and ethylene glycol (high temperature) standards. The exchange rate k was determined by line shape analysis using gNMR.[36] Plotting $R\ \ln(kh/k_BT)$ vs $1/T$ gave the activation enthalpies and entropies for the amidinate rearrangement of the compounds (see Supporting Information).

X-ray Crystallographic Structure Determinations of 9 and 10. Diffraction data were measured on a Bruker X8 APEX-II kappa geometry diffractometer with Mo radiation and a graphite monochromator. Frames were collected at 100 K as a series of sweeps with the detector at 40 mm and 0.3 degrees between each frame and were recorded for 10 s. APEX-II[37] and SHELX-97[38] software were used in the collection and refinement of the models.

Crystals of **9** were colorless irregular fragments, and a sample sized 0.30 × 0.19 × 0.12 mm^3 was mounted for data collection. A total of 77316 reflections were counted, which averaged to 7546 independent data. Hydrogen atoms were placed in calculated positions. There is disorder in the tantalum position and in the ligand arrangement, which refined to an 81/19 distribution. The lower occupancy nitrogen and carbon sites were kept isotropic. The geometry is unreliable in the 19% conformer. The disorder propagates into the *tert*-butyl substituents, but we were unable to model a reasonable minor component in this region.

Crystals of **10** grew as yellow rods, and a sample with dimensions of 0.26 × 0.16 × 0.16 mm^3 was used for data collection. A total of 68661 reflections were measured, yielding 7255 unique data. Hydrogen atoms were placed in calculated positions. There is disorder in the tantalum and bromine positions, and a 3:1 occupancy was used to describe these atoms, and their alternate atoms labeled with prime designators. The tantalum atom is 0.501 Å away from its minor component, and bromine is 0.120 Å away from bromine. There are large thermal ellipsoids on the terminal methyl groups, due primarily to the shift in the disordered tantalum positions. Refining without the partial tantalum and bromine positions produced a large peak in the difference map of 20 electrons 0.7 Å from tantalum, and high R values of 0.11 and 0.26 for R and wR respectively. Reducing the symmetry of the space group to that of $P2(1)$ did not resolve the disorder.

For **2**, four data sets on crystals from different batches were collected, and all suffered from disorder and/or twinning. The maps clearly showed the correct molecule, but there was disorder in the tantalum position (~1 Å apart) and more serious disorder in the ligand arrangement. No satisfactory model was obtained suitable for publication despite twinning solution attempts and partial atom occupancies techniques.

Acknowledgment. We thank the Army Research Office (Grant W911NF-07-0489) for generous support of this research.

Supporting Information Available: Tables of rates of amidinate rearrangement and plots of $R\ \ln(kh/k_BT)$ versus $1/T$ for complexes **2**, **9**, and **10** (4 pages). X-ray crystallographic files in CIF format for the structure determinations of **9** and **10**. This material is available free of charge via the Internet at http://pubs.acs.org.

---

[36] *gNMR*; Adept Scientific PLC: Amor Way, Letchworth, Herts, SG6 IZA, U.K., 2000.

[37] *APEX II collection and processing programs*, distributed by the manufacturer; Bruker AXS Inc.: Madison WI, 2005.

[38] Sheldrick, G. *SHELX-97*; University of Göttingen: Göttingen, Germany, 1997.